frontiers in Materials

ORIGINAL RESEARCH
published: 27 January 2021
doi: 10.3389/fmats.2020.595437

High-Sensitivity Refractive Index Sensor Based on a Cascaded Core-Offset and Macrobending Single-Mode Fiber Interferometer

*Chuanxin Teng[1], Yongjie Zhu[1], Fangda Yu[2], Shijie Deng[1], Libo Yuan[1], Jie Zheng[3] and Yu Cheng[1]**

[1]Guangxi Key Laboratory of Optoelectronic Information Processing, Guilin University of Electronic Technology, Guilin, China, [2]College of Electrical and Information Engineering, Beihua University, Jilin, China, [3]State Key Laboratory on Integrated Optoelectronics, College of Electronic Science and Engineering, Jilin University, Changchun, China

A high-sensitivity Mach–Zehnder interferometer (MZI) based on the cascaded core-offset and macrobending fiber structure is proposed for refractive index (RI) measurement. The core-offset structure makes the fiber core mode couple to the cladding modes, and some of them recouple back to the fiber core at the macrobending structure forming a model interference effect. The liquid RI can be measured by monitoring the spectral shift of the modal interference. The RI sensing performances for the interferometers with different macrobending radii and core offsets are investigated experimentally. Experimental results show that when the core offset is 2 μm and the macrobending radius is 5.5 mm, the sensitivity can reach 699.95 nm/RIU for the RI of 1.43. The temperature dependence for the proposed sensor is also tested, and a temperature sensitivity of 0.112 nm/°C is obtained.

Keywords: cascaded core-offset and macrobending structure, high sensitivity, Mach–Zehnder interferometer, refractive index measurement, optical fiber sensor

OPEN ACCESS

Edited by:
Jin Li,
Northeastern University, China

Reviewed by:
Haifeng Hu,
University of Shanghai for Science and Technology, China
Daniel Jauregui-Vazquez,
University of Guanajuato, Mexico

****Correspondence:***
Yu Cheng
chengyu@guet.edu.cn

Specialty section:
This article was submitted to Smart Materials, a section of the journal Frontiers in Materials

Received: *16 August 2020*
Accepted: *23 November 2020*
Published: *27 January 2021*

Citation:
Teng C, Zhu Y, Yu F, Deng S, Yuan L, Zheng J and Cheng Y (2021) High-Sensitivity Refractive Index Sensor Based on a Cascaded Core-Offset and Macrobending Single-Mode Fiber Interferometer. Front. Mater. 7:595437. doi: 10.3389/fmats.2020.595437

INTRODUCTION

The measurement of liquid refractive index (RI) plays an important role in many areas, such as food safety, environmental monitoring, and medical diagnosis. Optical fiber-based RI sensors have the advantages of immunity to electromagnetic interference, compact size, high sensitivity, fast response, resistant to corrosion, and available for remote sensing (Li et al., 2017a; Li et al., 2017b). To date, many kinds of optical fiber-based RI sensors have been proposed, for example, the optical fiber Bragg grating-based RI sensor (Tian et al., 2019), the optical fiber surface plasmon resonance-based RI sensor (Zhao et al., 2014), the optical fiber long-period grating-based RI sensor (Zhao et al., 2020), and so on. For fabricating the fiber gratings, the phase masks and photolithographic procedures are needed to be implemented, and a metal coating process is required for the surface plasmon resonance-based RI sensors; however, these fabrication processes are costly and time consuming. In the recent years, the in-line fiber Mach–Zehnder interferometers (MZIs) have attracted more and more attention due to their advantages of low cost and easy fabrication. Various configurations of fiber-based MZIs have been reported including the two core-offset fiber structure (Tian and Yam, 2009), the two tapered fiber structure (Wang et al., 2016), the two peanut fiber structure (Wu et al., 2012), the two microcavities fiber structure (Wang et al., 2009b), and so on. However, the sensitivities for these structures-based RI sensors are not high enough; although by reducing the fiber diameter

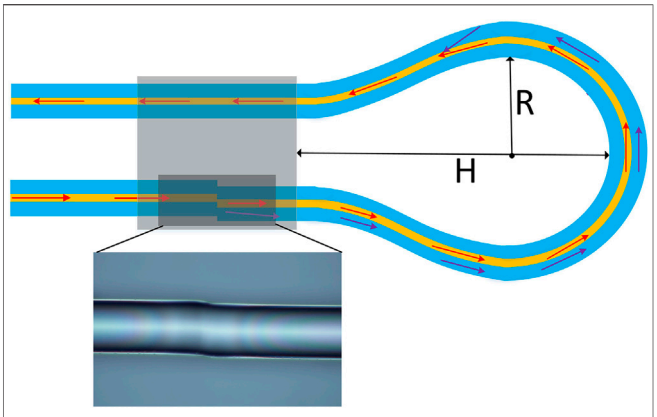

FIGURE 1 | The schematic illustration of the sensor structure.

via chemically etching or tapering could improve the sensitivity (Huang et al., 2008; Gao et al., 2013), this makes the sensor fragile and significantly reduces the mechanical strength of the sensors.

Bending optical fiber is a simple and effective method to fabricate optical fiber RI sensors, which could achieve high sensitivity and maintain the good mechanical strength. Recently, several bent single-mode fiber-based RI sensors have been presented (Wang et al., 2009a; Ladicicco et al., 2011; Zhang and Peng, 2015a; Zhang and Peng, 2015b; Zhang et al., 2015; Fang et al., 2016; Liu et al., 2016; Gong et al., 2017; Yu et al., 2019). Wang et al. (2009a) proposed an intensity demodulated RI sensor based on the macrobending single-mode fiber; however, the intensity demodulated sensor is easily affected by the fluctuation of light source and the external environments. Later, some wavelength demodulated RI sensors based on the bent fiber were proposed. Zhang and Peng, (2015b) presented an optical fiber refractometer by using the leaky-mode interference from bent fiber, and its sensitivity reached 204 nm/RIU. In the same year, the same group employed two U-shaped structure fibers with different macrobending radii to realize a dual-channel optical fiber refractometer, and the RI sensitivity can reach 245 nm/RIU (Zhang and Peng, 2015a). Liu et al., (2016) proposed a balloon-like fiber interferometer for RI and temperature measurement, and the RI sensitivity reached 225.95 nm/RIU. Yu et al. (2019) improved the sensitivity of the core-offset fiber structure MZI by bending, and a sensitivity of 358.039 nm/RIU was obtained. Besides, in order to realize the temperature compensation, some researchers introduced the grating structure to the bent fiber-based refractometer (Zhang et al., 2015; Gong et al., 2017).

In this research, a high-sensitivity optical fiber interferometer based on the cascaded core-offset and macrobending fiber structure is proposed and demonstrated. An MZI is proposed for RI sensing by cascading a core-offset and a macrobending structure fiber with a selected macrobending radius. The liquid RI can be measured by monitoring the spectral shift of the modal interference. The RI sensing performances for the sensor probes with different macrobending radii and core offsets are investigated experimentally. The results show that a sensitivity of 699.95 nm/RIU can be achieved for the probe with a 2 μm core offset and 5.5 mm macrobending radius when the RI is 1.43. And, in the temperature range of 35–65°C, a temperature sensitivity of 0.112 nm/°C is obtained. The sensor proposed has the advantages of high sensitivity, simple configuration, easy fabrication, and low cost.

SENSOR STRUCTURE AND OPERATION PRINCIPLE

The schematic illustration of the sensor structure is shown in **Figure 1**. A commercial, standard single-mode fiber is used to fabricate the cascaded core-offset and macrobending structure. The core-offset structure was fabricated by splicing two fibers with some core offset and packaged in a heated shrinkable tube. Then, the packaged core-offset fiber was inserted and fixed into another shrinkable tube; by putting the other end of the fiber into the tube as well, the macrobending structure can be formed. As shown in **Figure 1**, R is the macrobending radius, H is the distance between the macrobending top and the shrinkable tube end, and the value of H varies with R. To improve the interference visibility and the interaction between the measured liquid and optical signal, the coating of the bending section of the fiber should be stripped off. The core-offset structure of single-mode fiber could split the light into two parts: one of them is the fundamental core mode propagating in the fiber core and the other one is the cladding modes propagating in the fiber cladding; the different optical paths of the residual core mode and cladding modes could form an intermodal MZI. The transmission spectrum of the interferometer is simply expressed as that of a two-mode interference:

$$I = I_{co} + I_{cl} + 2\sqrt{I_{co}I_{cl}}\cos\phi\,, \tag{1}$$

where I is the light intensity of the output light, I_{co} and I_{cl} are the intensities of the core and cladding mode, respectively, and ϕ is the phase difference of the two interference modes, which can be expressed as

$$\phi = \frac{2\pi\,(n_{co} - n_{cl})L_{eff}}{\lambda}, \tag{2}$$

where n_{co} and n_{cl} are the effective RIs of the optical fiber core and cladding, respectively, L_{eff} is the effective length of the two mode interference paths, which depends on the fiber length of coating-stripped region after the core-offset structure, and λ is the wavelength in vacuum. When $\phi = (2i+1)\,\pi$, i is a positive integer, the interference dip appears, and the wavelength dip can be expressed as

$$\lambda_i = \frac{2\,(n_{co} - n_{cl})L_{eff}}{2i+1}. \tag{3}$$

From **Eq. 3**, it can be seen that for the fixed interference path length, the position of the interference dip depends on the effective RI difference between the core and the cladding mode. When the external environment RI changes, the effective RI of the cladding mode will change, while the effective RI of the fiber core mode will not change, which will lead to the change in the position of the wavelength dip.

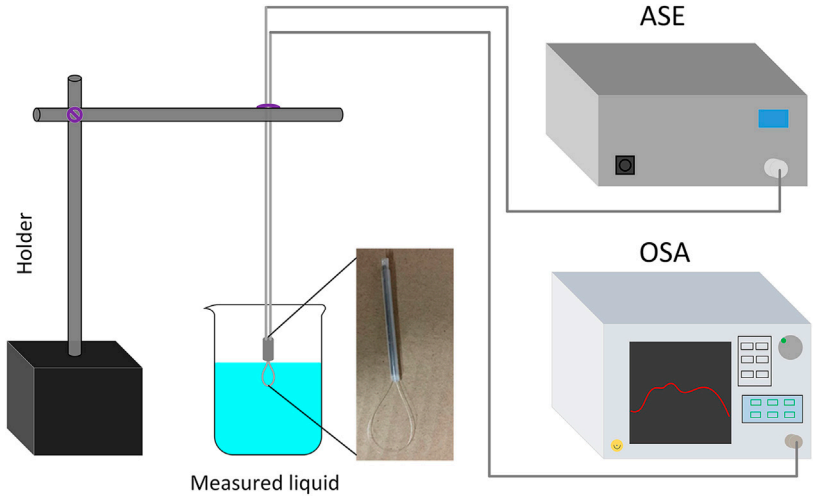

FIGURE 2 | The schematic of the experiment setup.

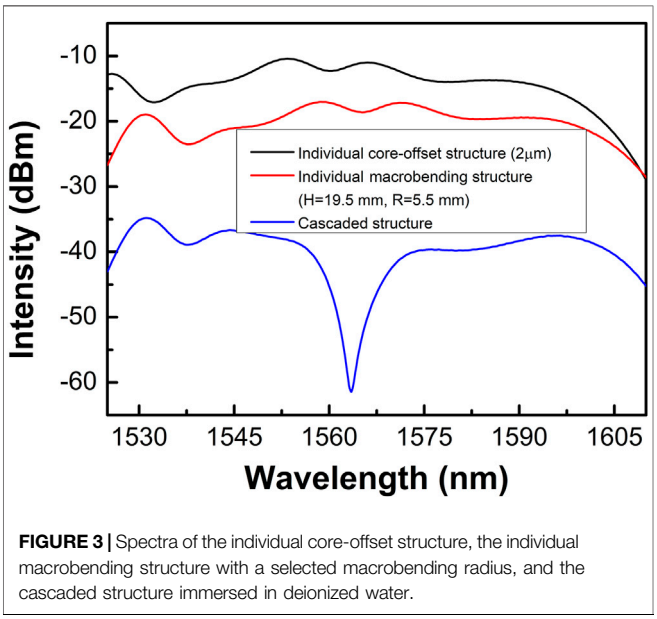

FIGURE 3 | Spectra of the individual core-offset structure, the individual macrobending structure with a selected macrobending radius, and the cascaded structure immersed in deionized water.

Therefore, the liquid RI can be detected by monitoring the changes of the wavelength dip.

EXPERIMENTS AND DISCUSSION

The schematic of the experiment setup is shown in **Figure 2**. A broadband light source (ASE) (A-0002, HOYATEC, Shenzhen, China) with the wavelength range of 1525–1610 nm was connected into the fiber input end (near the core-offset port), and an optical spectrum analyzer (OSA) (AQ6370D, YOKOGAWA, Tokyo, Japan) with a highest spectral resolution of 0.02 nm was used to record the transmission spectrum. By varying the concentration of glycerin, the water-glycerin solutions with different RIs of 1.34–1.43 and step of 0.01 were prepared as the measured liquids, and the RIs were measured by using an Abbe refractometer. The experiment was performed at the room temperature of 25 ˚C, and the whole macrobending structure was immersed into the measured liquid when the experiment was carried out.

Figure 3 shows the transmission spectra of the individual core-offset structure fiber, the individual macrobending structure fiber with a selected macrobending radius, and the cascaded structure fiber immersed in deionized water. From **Figure 3**, it is found that there is an obvious wavelength dip at 1563.5 nm with a resonance depth of about 22 dB on the transmission spectrum for the cascaded core-offset and macrobending structure; however, the wavelength dips are not obvious for the individual core-offset or the individual macrobending structure fiber with the same macrobending radius. This is because that for the individual core-offset structure, only a few of the cladding modes power couple with the core mode, and for the individual bending structure with the macrobending radius of 5.5 mm, the power of the cladding modes is small, which will reduce the visibility of the resonance dip.

Figure 4 shows the RI sensing performances for the probe with 2 μm core-offset and different macrobending radii of 3.6, 4.7, and 5.5 mm, respectively. It can be seen that as the RI increases, the wavelength dip has a red shift, and as the macrobending radius decreases, some more wavelength dips will appear, and the transmission loss will increase. This is because that as the macrobending radius decreases, more cladding modes will generate and recouple back to the fiber core, interfering with the fundamental core mode. It can be also seen that the intensity of spectra dip changes with the environment RI; they show a similar trend of increase first and then decrease. This may be because that the power of the dominant cladding mode which couples with the core mode increases first and decreases later as the environment RI increases. Therefore, the intensity demodulation can be also implemented to the proposed sensor

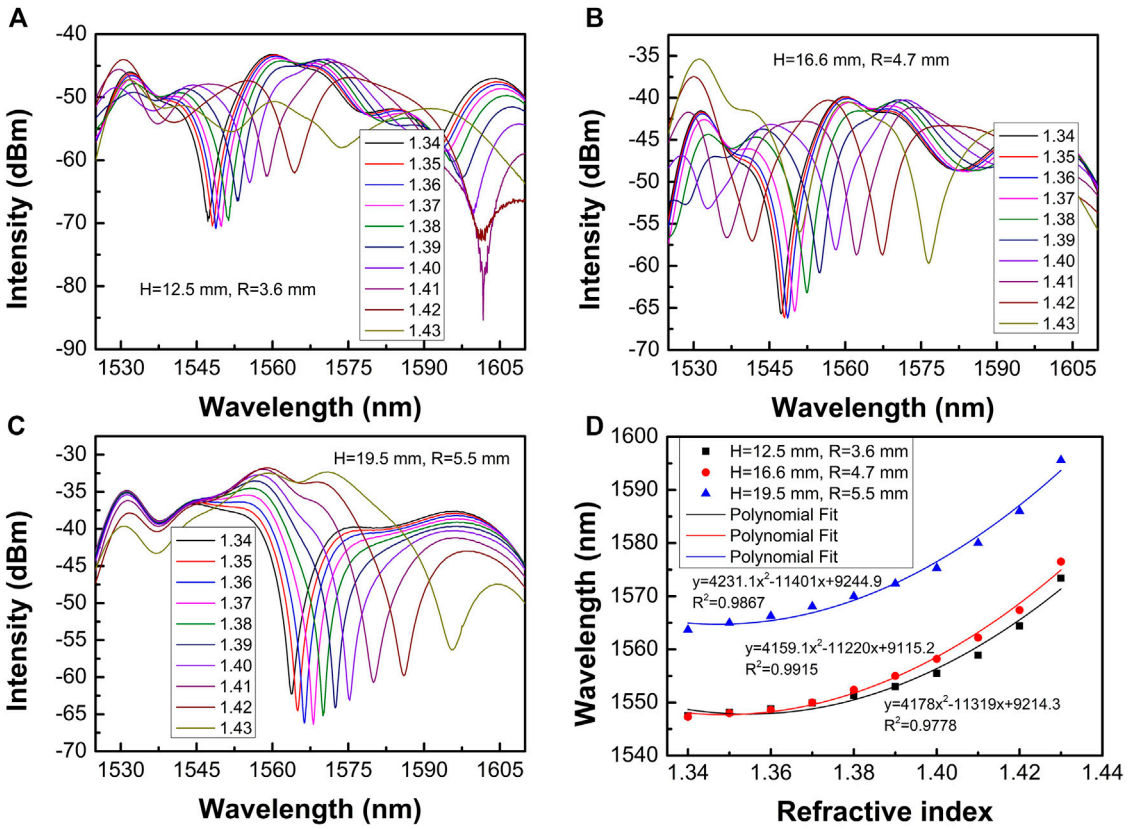

FIGURE 4 | The RI sensing performances for the probe with 2 μm core offset and different macrobending radii of 3.6 **(A)**, 4.7 **(B)**, and 5.5 mm **(C)**, respectively; **(D)** the wavelength shifts as a function of the measurement RIs.

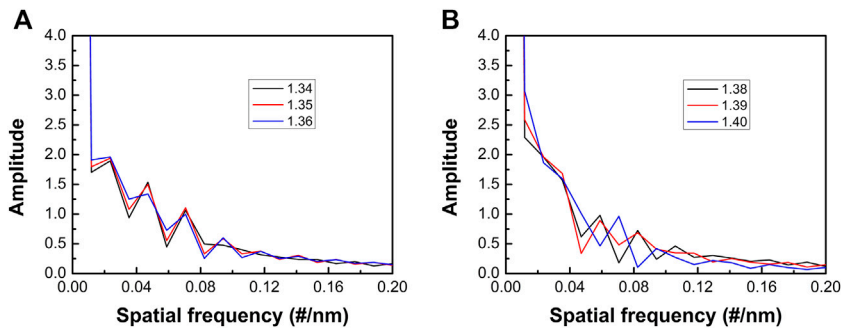

FIGURE 5 | Spatial frequency spectrum of the cascaded structure fiber probe with the core-offset of 2 μm and macrobending of 5.5 mm in different environment RI.

in some certain RI range. **Figure 4D** shows the wavelength dip shifts as a function of the measured RIs; it is found that the wavelength changes nonlinear with the RI increases for all the probes. The sensitivity S can be determined as

$$S = \frac{\Delta\lambda}{\Delta n}, \tag{4}$$

where $\Delta\lambda$ is the changes of the wavelength and Δn is the changes of liquid RI. By polynomial fitting, a high sensitivity of 699.95 nm/RIU can be achieved when the RI is 1.43 for the probe with the macrobending radius of 5.5 mm, which is higher than those in the reports of (Zhang and Peng, 2015a; Zhang and Peng, 2015b; Zhang et al., 2015a; Liu et al., 2016; Yu et al., 2019). This is because that the core-offset structure could excite the higher

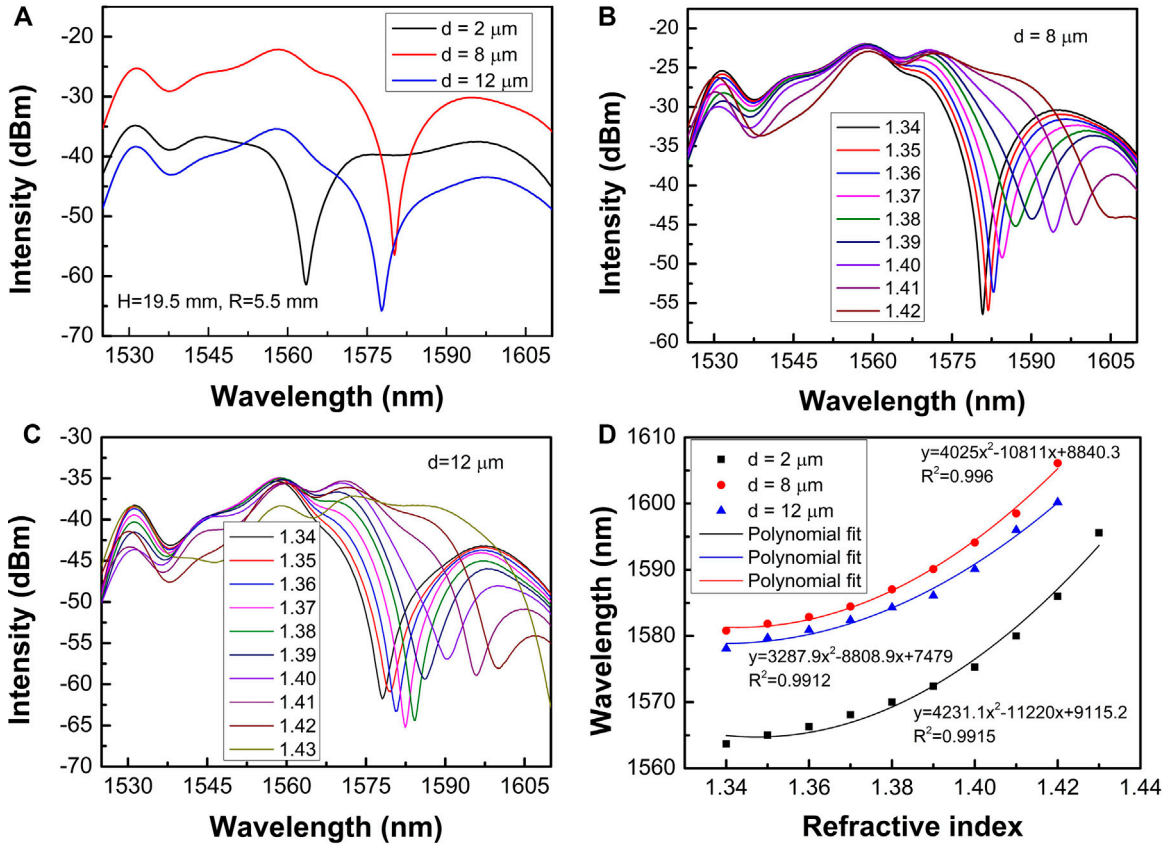

FIGURE 6 | (A) The transmission spectra of the probes with the macrobending radius of 5.5 mm and different core offsets in water; the RI sensing performance for the probe with the core-offset of 8 μm **(B)** and 12 μm **(C)**; **(D)** the wavelength shifts as a function of the measurement RIs.

order cladding modes, which are more sensitive to the environment RI.

In order to determine the cladding modes that construct the interference, the fast Fourier transform (FFT) of the wavelength spectrum is performed to get its corresponding spatial frequency spectrum for the cascaded structure fiber probe in different environment RI. The core-offset and the macrobending radius for the probe are 2 μm and 5.5 mm, respectively. As shown in **Figure 5A**, there is a dominant cladding mode contributing to the interference spectrum, whose peak presents at 0.02 nm^{-1}, and there are some other peaks present at about 0.04, 0.07, and 0.09 nm^{-1} when the environment RI is 1.34–1.36. It can be also found that the amplitude of the dominant cladding mode peak increases as the RI increases from 1.34 to 1.36. **Figure 5B** shows the spatial frequency spectrum when the environment RI is 1.38–1.40. It can be seen that the dominant cladding mode disappears, and some new peaks appear at about 0.06 and 0.08 nm^{-1} when the environment RIs are 1.38 and 1.39, and the amplitude for the peak of 1.38 is larger than that of 1.39. When the environment RI is 1.40, the locations of the peaks are different from the situations of 1.38 and 1.39, and the height of the peak becomes lower.

The influence of the core offset on the RI sensing performance is tested experimentally. **Figure 6A** shows the transmission spectra of the probes with different core offset of 2, 8, and 12 μm and the same macrobending radius of 5.5 mm in water. It can be seen that the probes with core offsets of 8 and 12 μm have a better visibility of the wavelength dip than that of the probe with core offset of 2 μm. **Figures 6B,C** show the RI sensing performances for the probes with core offsets of 8 and 12 μm in the RI range of 1.34–1.43, respectively. It can be seen from **Figures 6B,C** that as the RI increases, both of the wavelength dips have a red shift; however, for the liquid RI of 1.43, the wavelength dip cannot be determined precisely for the probes with core offsets of 8 and 12 μm. This may be because that a larger core offset will introduce more transmission loss. It can be also found that the intensity dip for the probe with the core offset of 8 μm has an obvious change in the RI range of 1.35–1.38; after a linear fit, a sensitivity of 366.78 dB/RIU is obtained, which is much higher than that reported in the literature (Liu et al., 2016). The wavelength dip shifts as a function of the measured RIs for the probes with different core offsets are shown in **Figure 6D**.

The temperature influence for the probe was also tested. **Figure 7** shows the temperature dependence for the probe with the core offset of 2 μm and macrobending radius of 3 mm. The experiment was carried out when the probe was immerged into the water bath with temperature changes from 65 to 35 °C, and the data of the transmission spectrum were recorded every 5 °C. A thermometer was used to monitor the temperature around the probe in real time. It can be seen from **Figure 7A** that as the

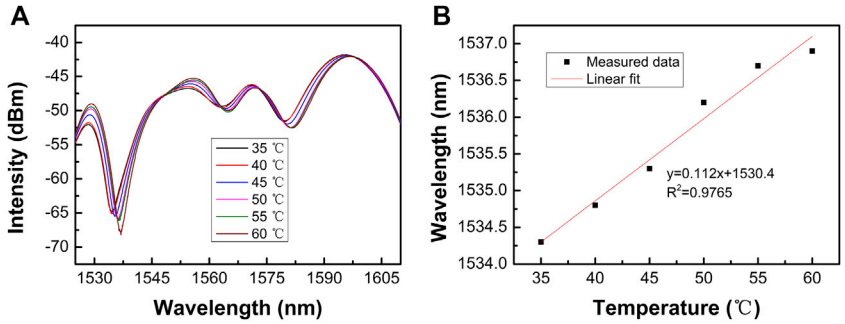

FIGURE 7 | The transmission spectrum of the probe in water with the temperature variations of 65–35°C **(A)** and the wavelength shifts as a function of the temperature variations **(B)**.

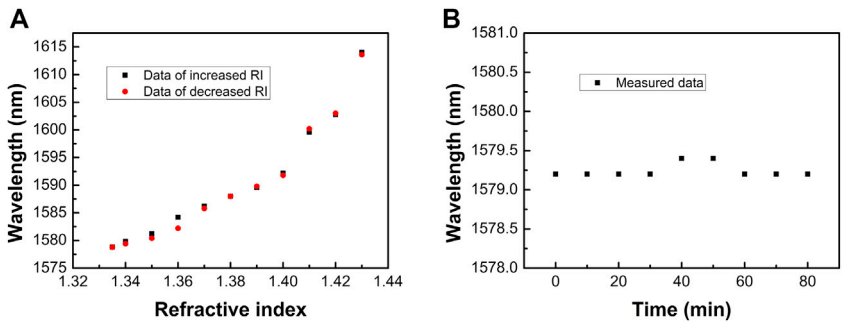

FIGURE 8 | The hysteresis **(A)** and stability **(B)** testes for the probe with a core-offset of 3 μm and macrobending radius of 5.5 mm.

TABLE 1 | A comparison between the proposed fiber RI sensor and other fiber-based RI sensors.

Sensor structure	Measurement range	Sensitivity	Modulation	Reference
Fiber Bragg grating	1.41–1.44	8.9 nm/RIU	Wavelength	Tian et al., (2019)
Two core-offset structure	1.315–1.3618	33.3 nm/RIU	Wavelength	Tian and Yam, (2009)
Cascaded fiber taper	1.33–1.792	158.4 nm/RIU	Wavelength	Wang et al., (2016)
Permanently bent fiber	1.33–1.3465	36.6%/RIU	Intensity	Ladicicco et al., (2011)
Macrobending fiber	1.4586–1.5396	Not mentioned	Intensity	Wang et al., (2009a)
Two bending regions fiber	1.3288–1.3696	204 nm/RIU	Wavelength	Zhang and Peng, (2015b)
Two different U-shaped fiber	1.3403–1.3726	207 nm/RIU and 245 nm/RIU	Wavelength	Zhang and Peng, (2015a)
Balloon-like fiber	1.3493–1.3822	225.95 nm/RIU	Wavelength	Liu et al., (2016)
Bending core-offset fiber interferometer	1.33–1.37	358.039 nm/RIU	Wavelength	Yu et al., (2019)
Long-period grating and bent fiber	1.3269–1.3721	183.4 nm/RIU	Wavelength	Zhang et al., (2015)
Cascaded core-offset and macrobending fiber	1.33–1.43	699.95 nm/RIU (RI = 1.43)	Wavelength	This work

temperature decreases, the wavelength dip shows a blue shift. **Figure 7B** shows the wavelength shifts as a function of the temperature variations; from a linear fit, it can be obtained that the temperature sensitivity is 0.112 nm/°C. The temperature sensitivity may be due to the thermal optic effects of the probe and measured liquid.

Figure 8A shows a reversed cycled RI measurement for the sensor with a core-offset of 3 μm and macrobending radius of 5.5 mm. It can be seen that the dip wavelength shifted to the shorter wavelengths when RI decreased. It can also be seen that most of the measured data are almost the same, which indicates the hysteresis for the sensor is small. **Figure 8B** shows the stability test results for this probe in deionized water; the data were recorded every 10 min; it can be seen that the stability of the sensor is good.

Table 1 shows the performance comparisons of the proposed fiber RI sensor with some of the fiber-based RI sensors referenced in this research. It shows that the proposed fiber RI sensor in this investigation has a comparable sensitivity and a larger measurement range.

CONCLUSION

In this research, a high-sensitivity RI sensor based on the cascaded core-offset and macrobending structure fiber MZI has been presented. The measurement RI can be detected by monitoring the shift of the wavelength dip. The RI sensing performances for the probes with different macrobending radii and core offsets are investigated experimentally. Experimental results show that the wavelength dip changes nonlinear with the RI variations. The results also show that as the macrobending radius decreases, the transmission loss will increase, and the RI measurement range will decrease for the probes with the macrobending radius of 5.5 mm and core offsets of 8 and 12 μm. When the core offset is 2 μm and the macrobending radius is 5.5 mm, the sensitivity of 699.95 nm/RIU is achieved for the RI of 1.43. The experimental results also show that the intensity demodulation can be also implemented to the proposed sensor in some certain RI range, and when the core offset is 8 μm and the macrobending radius is 5.5 mm, a high sensitivity of 366.78 dB/RIU is obtained in the RI range of 1.35–1.38. Finally, the temperature dependence, the hysteresis, and the stability of the sensor probe are analyzed. From the experiment, a temperature sensitivity of 0.112 nm/°C is obtained, the hysteresis for the sensor is small, and the sensor has a good stability.

DATA AVAILABILITY STATEMENT

The raw data supporting the conclusions of this article will be made available by the authors, without undue reservation.

AUTHOR CONTRIBUTIONS

CT was responsible for conceptualization; CT, YZ, and FY were involved in formal analysis; CT and FY performed investigation; LY and YC were responsible for resources; CT and YZ were responsible for visualization; CT, YZ, and SD wrote original draft; CT and SD wrote, reviewed, and edited the manuscript.

FUNDING

This research was funded by the National Key Research and Development Program of China, grant no. 2019YFB2203903; National Natural Science Foundation of China, grant nos. 61805050, 61965009, 61975038, 61827819, 61735009, 61964005, and 61705050; and National Natural Science Foundation of Guangxi, grant nos. 2018GXNSFBA281148 and 2019GXNSFBA245057.

REFERENCES

Fang, Y., Wang, C., and Chiang, C. (2016). A small U-shaped bending-induced interference optical fiber sensor for the measurement of glucose solutions. *Sensors* 16, 9. doi:10.3390/s16091460

Gao, S., Zhang, W., Bai, Z., Zhang, H., Geng, P., Lin, W., et al. (2013). Ultrasensitive refractive index sensor based on microfiber-assisted U-shape cavity. *IEEE Photon. Technol. Lett.* 25, 18. doi:10.1109/LPT.2013.2274492

Gong, Z., Chen, K., Zhou, X., and Yu, Q. (2017). Temperature-compensated refractive index sensor based on bent-fiber interference. *Opt. Fiber Technol.* 36, 6–9. doi:10.1016/j.yofte.2017.01.011

Huang, X., Chen, Z., Shao, L., Cen, K., Sheng, D., Chen, J., et al. (2008). Design and characteristics of refractive index sensor based on thinned and microstructure fiber Bragg grating. *Appl. Optic.* 47, 4. doi:10.1364/AO.47.000504

Ladicicco, A., Paladino, D., Campopiano, S., Bock, W., Cutolo, A., and Cusano, A. (2011). Evanescent wave sensor based on permanently bent single mode optical fiber. *Sensor. Actuator. B Chem.* 155, 2. doi:10.1016/j.snb.2011.01.021

Li, J., Chen, F., Li, H., Hu, H., and Zhao, Y. (2017a). Investigation on high sensitivity RI sensor based on PMF. *Sensor. Actuator. B Chem.* 242, 1021–1026. doi:10.1016/j.snb.2016.09.151

Li, J., Li, H., Hu, H., and Yao, C. (2017b). Refractive index sensor based on silica microfiber doped with Ag microparticles. *Optic Laser. Technol.* 94, 40–44. doi:10.1016/j.optlastec.2017.03.024

Liu, X., Zhao, Y., Lv, R., and Wang, Q. (2016). High sensitivity balloon-like interferometer for refractive index and temperature measurement. *IEEE Photon. Technol. Lett.* 28, 13. doi:10.1109/LPT.2016.2554624

Tian, P., Zhu, Z., Wang, M., Ye, P., Yang, J., Shi, J., et al. (2019). Refractive index sensor based on fiber Bragg grating in hollow suspended-core fiber. *IEEE Sensor. J.* 19, 24. doi:10.1109/JSEN.2019.2938786

Tian, Z., and Yam, S. (2009). In-line single-mode optical fiber interferometric refractive index sensors. *J. Lightwave Technol.* 27, 13. doi:10.1109/JLT.2008.2007507

Wang, P., Semenova, Y., Wu, Q., Farrell, G., Ti, Y., and Zheng, J. (2009a). Macrobending single-mode fiber-based refractometer. *Appl. Optic.* 48, 31. doi:10.1364/AO.48.006044

Wang, Y., Wang, D., Yang, M., Hong, W., and Lu, P. (2009b). Refractive index sensor based on a microhole in single-mode fiber created by the use of femtosecond laser micromachining. *Optic Lett.* 34, 21. doi:10.1364/OL.34.003328

Wang, Q., Wei, W., Guo, M., and Zhao, Y. (2016). Optimization of cascaded fiber tapered Mach–Zehnder interferometer and refractive index sensing technology. *Sensor. Actuator. B Chem.* 222, 159–165. doi:10.1016/j.snb.2015.07.098

Wu, D., Zhu, T., Chiang, K., and Deng, M. (2012). All single-mode fiber Mach–Zehnder interferometer based on two peanut-shape structures. *J. Lightwave Technol.* 30, 5. doi:10.1109/JLT.2011.2182498

Yu, F., Xue, P., and Zheng, J. (2019). Enhancement of refractive index sensitivity by bending a core-offset in-line fiber mach–zehnder interferometer. *IEEE Sensor. J.* 19, 9. doi:10.1109/JSEN.2019.2892718

Zhang, X., and Peng, W. (2015a). Bent-fiber intermodal interference based dual-channel fiber optic refractometer. *Optic Express* 23, 6. doi:10.1364/OE.23.007602

Zhang, X., and Peng, W. (2015b). Fiber optic refractometer based on leaky-mode interference of bent fiber. *IEEE Photon. Technol. Lett.* 27, 1. doi:10.1109/LPT.2014.2359227

Zhang, X., Xie, L., Zhang, Y., and Peng, W. (2015). Optimization of long-period grating-based refractive index sensor by bent-fiber interference. *Appl. Optic.* 54, 31. doi:10.1364/AO.54.009152

Zhao, Y., Deng, Z., and Wang, Q. (2014). Fiber optic SPR sensor for liquid concentration measurement. *Sensor. Actuator. B Chem.* 192, 229–233. doi:10.1016/j.snb.2013.10.108

Zhao, Y., Liu, S., Luo, J., Chen, Y., Fu, C., Xiong, C., et al. (2020). Torsion, refractive index, and temperature sensors based on an improved helical long period fiber grating. *J. Lightwave Technol.* 38, 8. doi:10.1109/JLT.2019.2962898

Conflict of Interest: The authors declare that the research was conducted in the absence of any commercial or financial relationships that could be construed as a potential conflict of interest.